

RSC Advances



This is an *Accepted Manuscript*, which has been through the Royal Society of Chemistry peer review process and has been accepted for publication.

Accepted Manuscripts are published online shortly after acceptance, before technical editing, formatting and proof reading. Using this free service, authors can make their results available to the community, in citable form, before we publish the edited article. This *Accepted Manuscript* will be replaced by the edited, formatted and paginated article as soon as this is available.

You can find more information about *Accepted Manuscripts* in the [Information for Authors](#).

Please note that technical editing may introduce minor changes to the text and/or graphics, which may alter content. The journal's standard [Terms & Conditions](#) and the [Ethical guidelines](#) still apply. In no event shall the Royal Society of Chemistry be held responsible for any errors or omissions in this *Accepted Manuscript* or any consequences arising from the use of any information it contains.

ARTICLE

Solvent Effect on Electron and Proton Transfer in the Excited State of Hydrogen Bonded Phenol-Imidazole Complex

Cite this: DOI: 10.1039/x0xx00000x

Baotao Kang,^{a,†} Hu Shi,^{a,†} Shihai Yan,^{b,*} Jin Yong Lee^{a,*}Received 00th XXX, XXX,
Accepted 00th XXX, XXX

DOI: 10.1039/x0xx00000x

www.rsc.org/

Density functional theory calculations have been carried out for the ground state (S_0) and the first excited state (S_1) of the H-bonded phenol and imidazole complex as a model system for the active site of photosystem II. Potential energy surfaces (PES) of S_0 and S_1 along proton transfer coordinate were obtained. Based on the relative stability and small energy barrier for proton transfer, it was found that proton transfer could take place in the excited state both in vacuum and in water. As confirmed by the charge distribution, the proton transfer is determined to be coupled with electron transfer (PCET) in vacuum, while not in water. Such phenomenon should originate from the solvent effect stabilizing π^* state with large dipole moment, which results in a different structure of product.

Introduction

Electron transfer and proton transfer play fundamental roles in chemistry and biology. These two processes occur simultaneously in some systems and have been the subjects of extensive experimental and theoretical efforts.¹⁻⁸ These processes can be classified into three types based on the mode of electron and proton movement: hydrogen atom transfer (HAT), electron coupled proton transfer (ECPT) or proton coupled electron transfer (PCET), and separated electron transfer and proton transfer (ET+PT). When the transport distance is short, electron and proton may transfer together. Among the three types of electron and proton transfer processes, PCET is especially prevalent for metallo-cofactors, which can activate substrates at carbon, oxygen, nitrogen and sulfur atoms. PCET is an important charge transport pathway in various biochemical, electrochemical, and small-molecule organic and inorganic reactions. The proteins and enzymes of photosynthesis and respiration have optimized structures that function by utilizing energy gathered along a charge-separating network to drive a proton pump, which in turn is manifest in a transmembrane chemical potential to provide energy for the synthesis of complex biomolecules.^{3,9-11} In photosystem II (PS II), an electron of tyrosine transfers to P680⁺ upon oxidation, in conjugation with a proton transfer from tyrosine to an adjacent base. In this process, one electron is detached from a nearby metal cluster and is transferred to tyrosine while deprotonation takes place in a concerted fashion between tyrosine and water.^{12,13} However, the mechanisms of some processes regarding types of electron and proton transfer are controversial. For the wild type of *Synechocystis* sp. PCC 6803 for instance, an electron transfer from Mn to Tyr 161 accompanied by proton transfer from Mn-OH₂ to His 190 has been proposed, whereas another mechanism supports proton transfer from Mn-OH₂ to Asp 61.¹⁴

An important example of PCET is observed in tyrosine/tyrosyl radicals.⁶ Tyrosine/tyrosyl radicals of PS II have received a great attention due to the diversity of radical types such as Tyr_D[•] and Tyr_Z[•] as well as the rapid kinetics of radical formation.^{15,16} Besides, being a protogenic amino acid tyrosine plays a special role by virtue of its phenol functionality. Phenol, also known as carboic acid, is the simplest aryl alcohol, and its ability to accept and donate both electrons and protons has been extensively investigated.¹⁷⁻¹⁹ It has been established that phenoxy radical (PhO[•]) provides an accurate structural and spectroscopic model for tyrosine phenoxy radical,²⁰ and its properties such as charge distribution, spin density, vibrations, and others have been intensively investigated.²¹ Phenol complexes with other simple molecules such as water, ammonia and bases²²⁻²⁷ have been used as valuable models that encompass hydrogen bonding, electron transfer, and proton pumping at the molecular level. Histidine, an integral amino acid residue in many important biological systems, can serve as a base or as a weak acid. Imidazole is often utilized as a model compound for histidine. The hydrogen-bonded complex of phenol and imidazole has been used as a model to study electron and proton transfer between tyrosine and histidine residues upon the oxidation of tyrosine in PS II.^{28,29} It has been confirmed that oxidation of the phenol-imidazole complex triggers spontaneous proton transfer from phenol to imidazole and subsequently the imidazole proton can further migrate to a distant acceptor pool.²⁴ However, to the best of our knowledge, there are no studies on the possible proton transfer by electronic excitation at the active site in PS II. Hence, density function theory (DFT) calculations were carried out to investigate the proton and electron transfer under photo excitation in vacuum and water solvent. The potential energy surface (PES) for the ground (S_0) and the first excited (S_1) states along the proton transfer coordinate was studied to investigate the detailed

mechanism. We found that proton transfer can take place in the excited state both in vacuum and water.

Computational Method

CAM-B3LYP with long range correction using Coulomb-attenuating method has been proved to work well in the systems involving charge transfer (CT) process during photo-excitation.³⁰⁻³² In the present paper, DFT calculations with CAM-B3LYP exchange functions were carried out. Structures of isolated phenol (PH), imidazole (IM), and the phenol-imidazole complex (PH-IM) were fully optimized with CAM-B3LYP employing the 6-311++G** basis sets. Geometries of the first excited state (S_1) were fully optimized by the time-dependent DFT (TD-DFT) calculation with the same basis set. The potential energy surfaces (PES) of S_0 and S_1 were obtained along the proton transfer coordinate without any restriction on other coordinates. Frequency calculations were performed to confirm the transition states or local minima.

For a chemical reaction, solvent effects have an important influence on the potential energy barrier, enthalpy difference, and so on. In the present study, Tomasi's polarizable continuum model (PCM) by self-consistent reaction field (SCRF) method was utilized to investigate the solvent effect on the electron/proton transfer. In PCM model, the cavity was defined as the union of a series of interlocking atomic spheres. The polarization effect of the solvent continuum was computed by numerical integration. In addition, water molecules may play a vital role in proton transfer processes. Thus, we carried out QM/MM calculations treating explicitly the water molecules in the first hydration shell. We encapsulated PH-IM with water box of 22 Å (about 3,300 water molecules) as demonstrated in Fig S1 in Electronic Supplementary Information, and optimized the structures by treating PH-IM and water molecules within 6 Å quantum mechanically and other water molecules by MM. Amber 12³³ software was employed in this simulation with TIP3P³⁴ potential for classical water molecules, QM for PH-IM, and PM3 for water molecules within 6 Å. Meanwhile the rests as MM part were dealt with Amber ff99SB force field.³⁴ The cutoff value for QM and MM parts was 6 Å and 8 Å, respectively. Temperature (300 K) was controlled by the Berendsen thermostat with coupling constants of 1.0 ps and the trajectory of last 200 ps was collected for further analysis. After optimization, we selected PH-IM and the water molecules in the first hydration shell (54 water molecules) and the structure was fully optimized by CAM-B3LYP /6-31+G*. Apart from QM/MM calculation, all calculations were performed using a suite of Gaussian 09 programs.³⁵

Results and Discussions

The excitation properties of the first two excited states corresponding to $\pi\pi^*$ and $\pi\sigma^*$ transitions, were investigated, and the corresponding molecular orbitals (MOs) of isolated PH are shown in Fig 1. The absorption wavelength (λ_{abs}) was estimated to be ~234 nm for the $\pi\pi^*$ transition, and ~220 nm for the $\pi\sigma^*$ transition which are comparable to the experimental values of 269 nm and 210 nm, respectively.^{36, 37} In the $\pi\sigma^*$ state, the diffused σ^* electron is largely localized on the phenolic hydrogen. As the O-H bond increases, the σ^* electron collapses to the 1s orbital of the phenolic hydrogen.³⁸ This process could induce an intermolecular CT. In addition, the first vertical excitation of imidazole in gas phase corresponds to a $\pi\sigma^*$ transition with λ_{abs} of 220 nm which is consistent with the

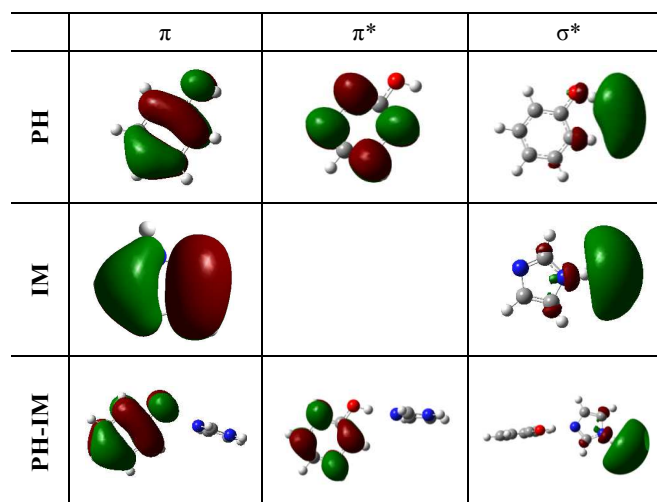


Fig 1. The molecular orbitals of isolated PH, IM and the PH-IM complex in vacuum.

values obtained by CASPT2 (217 nm³⁹). Phenol and imidazole form a complex (PH-IM) through hydrogen bonding. The bond length of O-H ($R_{\text{O-H}}$) slightly increases to 0.984 Å and $R_{\text{C-O}}$ decreases to 1.350 Å by forming hydrogen bonding. The $\pi\pi^*$ transition is a localized excitation (LE) on the phenol moiety, which is similar to that of the isolated phenol. And the second excited state corresponds to a CT state with the $\pi\sigma^*$ transition. The σ^* orbital of PH-IM is localized on the imidazole moiety rather than the O-H. With the formation of hydrogen bonded complex, the λ_{abs} of the $\pi\pi^*$ and $\pi\sigma^*$ transitions are slightly red-shifted to 245 nm (similar to that by CASSCF of 250 nm) and 227 nm.

Table 1. Some important structural parameters of the S_0 and S_1 (denoted with an asterisk) state for PH and PH-IM complex in both vacuum and water

Medium		$R_{\text{O-H}}$	$R_{\text{C-O}}$	$R_{\text{O-N}}$	$R_{\text{N-H}}$	\angle_{COH}
Vacuum	PH	0.961	1.364			110
	PH*	0.965	1.339			110
	PH-IM	0.984	1.350	2.801	1.821	112
	PH-IM*	1.008	1.320	2.686	1.681	113
	TS*	1.080	1.310	2.592	1.514	114
Water	P-HIM*	1.900	1.242	2.909	1.010	172
	PH-IM	1.000	1.351	2.715	1.718	113
	PH-IM*	1.050	1.308	2.575	1.528	115
	TS*	1.170	1.295	2.480	1.312	118
	P-HIM*	1.556	1.275	2.624	1.070	125

(The distance is given in the unit of Å and the angle was given in °)

The PESs of S_0 and S_1 for the complex in vacuum along the O-H coordinate were obtained (Fig 2). The PES of S_0 monotonically increases as the O-H distance increases, with only one local minimum (denoted as PH-IM). Whereas, the PES of S_1 shows a double well curve, where there are two minima (PH-IM* and P-HIM*) and one transition state (TS*) connecting them. In PH-IM* and P-HIM*, the proton exists in phenol and imidazole, respectively. From frequency calculation, TS* was confirmed to be a transition state because only one imaginary frequency (173 icm^{-1}) was observed with H moving to IM moiety. In addition, PH-IM* and P-HIM* can be considered as local minima without imaginary frequency (an

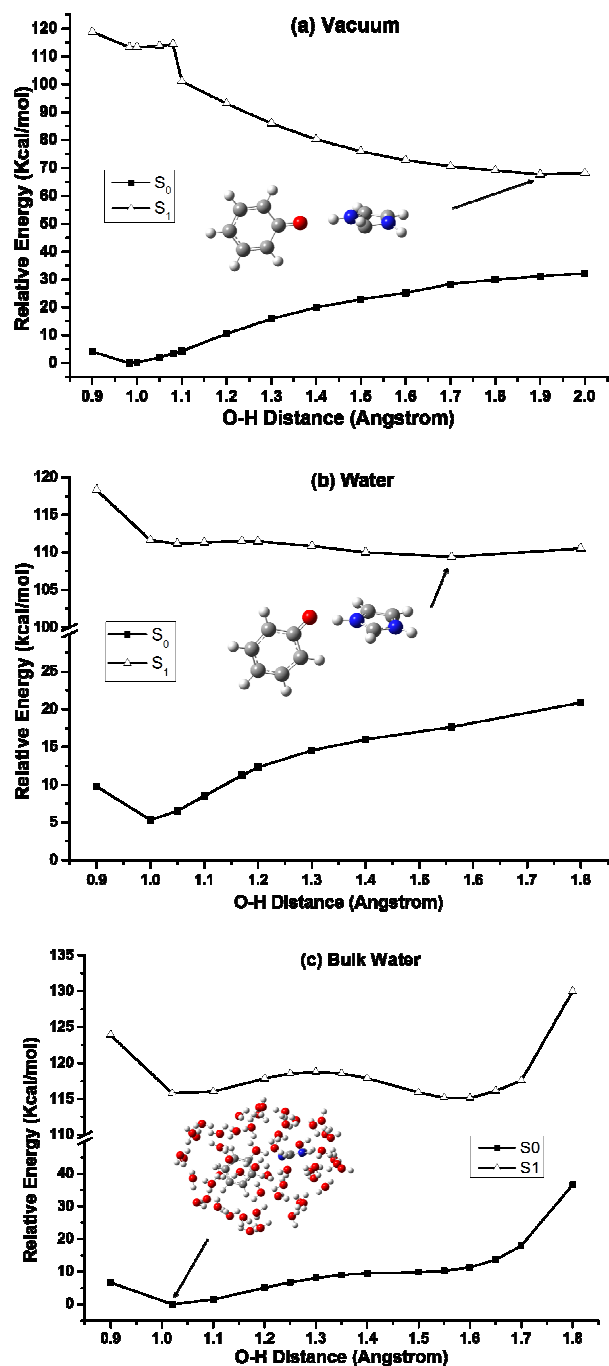


Fig 2. PES of S_0 and S_1 in (a) vacuum and (b) water by PCM model and (c) bulk water.

imaginary mode less 40 icm^{-1} for P-HIM* is negligible as usual). Some important structural parameters were listed in Table 1. Additionally, the behaviors of R_{O-N} and angle of C-O-H (\angle_{COH}) along proton transfer were studied and shown in supporting information. In vacuum, the O-H bond length (R_{O-H}) increased and C-O bond length (R_{C-O}) decreased upon excitation. The interatomic distances of O-N (R_{O-N}) and N-H (R_{N-H}) also decreased upon excitation, which implies a strengthened hydrogen bonding. For the transition state of the excited state (TS*), R_{O-H} was calculated to be 1.080 Å and R_{C-O}/R_{O-N} further decreased to 1.310/2.592 Å. After proton transfer from phenol to imidazole in the excited state (P-HIM*), R_{C-O}

decreased to 1.242 Å and R_{O-N} increased to 2.909 Å. It is worthy to note that the proton is localized along the C-O axis rather than the O-H axis of phenol, as reflected by the increased \angle_{COH} from 110° in PH-IM* to 172° in P-HIM* (Fig S2). Considering the relative stability and small barrier (1.09 kcal/mol), excited state proton transfer (ESPT) can take place in vacuum. Here we proposed that the proton affinity (PA) of imidazole plays an important role. First, it provides an abstraction force to detach the phenolic proton. Second, it can stabilize the proton transferred complex. For example, as reported earlier in phenol and water complex, PH-W* lies 18 kcal/mol below P-HW* along the PES, *i.e.* ESPT cannot take place. As the PA increases from 167 kcal/mol of water⁴⁰ to 204 kcal/mol of amonia⁴¹, P-HNH₃* becomes more stable than PH-NH₃* by about 1 kcal/mol, with a much reduced energy barrier of 9 kcal/mol. Here the PA of imidazole is 229 kcal/mol⁴², the P-HIM* in vacuum was much stabilized and the barrier further decreased to 1.09 kcal/mol.

Then the solvent effect via PCM model was taken into account. For isolated PH and IM, solvent shows a slight effect on the absorption properties. The λ_{abs} of the $\pi\pi^*$ and $\pi\sigma^*$ transitions were 237 nm and 210 nm for PH in water and that of $\pi\sigma^*$ transition for IM was 204 nm IM in water. The relative stability and energy barrier of the complex during the proton transfer are greatly influenced by environment such as external electric field and solvent polarity. When the solvent effect was included, the H-bonding of PH-IM is enhanced as evidenced by the interatomic distances. The R_{O-N} decreased by 0.086 Å to 2.715 Å, while R_{C-O} and R_{O-H} increased slightly by 0.016 Å and 0.001 Å to 1.000 Å and 1.351 Å, respectively. When solvent

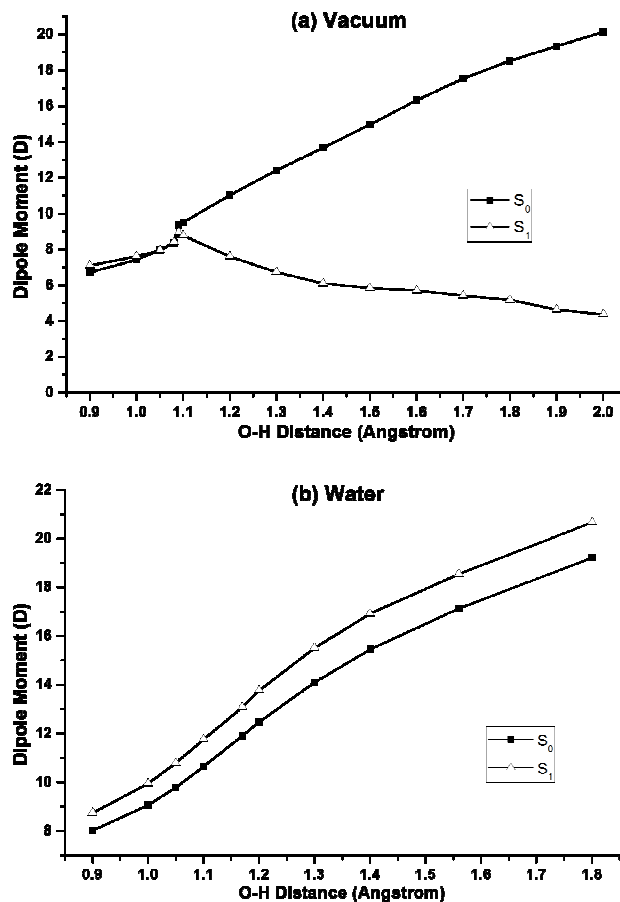


Fig 3. Dipole moment of S_0 and S_1 in (a) vacuum and (b) water.

effect was included, the absorption energies of PH-IM slightly changed to give the $\pi\pi^*$ transition of 243 nm and the $\pi\sigma^*$ transition of 216 nm, respectively. To investigate the solvent effect on the proton transfer reaction, the PESs of S_0 and S_1 were obtained considering the solvent medium by polarizable continuum model (PCM) method, and the results were displayed in Fig 2 (b). The S_0 PES in water is a single-well curve similar to that in vacuum. In contrast to the S_0 PES, the S_1 PES is a double-well curve. The two local minima along the S_1 PES were denoted by PH-IM* and P-HIM* depending on the occurrence of the phenolic proton, and the transition state was denoted by TS*. From frequency calculations, PH-IM* and P-HIM* have been proved to be local minima without any imaginary frequency, and TS* is real transition state with only one imaginary mode (789 icm^{-1}) with H moving to IM. Photoexcitation could enhance the H-bonding of PH-IM in water as reflected by the reduced R_{O-N} and R_{H-N} of PH-IM*. R_{O-N} and R_{H-N} decreased from 2.715 Å and 1.718 Å of PH-IM to 2.686 Å and 1.686 Å of PH-IM*, respectively. In addition, R_{C-O} decreased to 1.320 Å and R_{O-H} increased to 1.008 Å, implying a weakened phenolic O-H bond which is similar to those in vacuum. As the proton transfers to imidazole (P-HIM*), R_{O-N} further decreased to 2.624 Å. The R_{O-H} was 1.556 Å and the \angle_{COH} increased slightly from 118° of PH-IM* to 135° of P-HIM* (Fig S2). That is, the proton is located mostly along the O-H direction, which is different to that in vacuum. In water, for TS*, the phenolic proton is located nearly at the center of the phenolic O and the imidazole N, with R_{O-H1}/R_{H1-N1} of 1.170/1.312 Å, respectively. Moreover, R_{O-N} at the TS* is much reduced to 2.480 Å. From the PES, P-HIM* is energetically more stable than PH-IM* by 1.8 kcal/mol. With the consideration of the small energy barrier (0.4 kcal/mol), the ESPT can take place in water from PH-IM* to P-HIM*. Meanwhile for the reverse ESPT from P-HIM* to PH-IM*, the energy barrier slightly increases to 2.2 kcal/mol. The reverse ESPT should be possible to take place if some excess of energy was induced.

As shown in Fig 2 (c), in bulk water only one water was found to form H-bonding to the phenolic O atom which is consistent with a previous report.⁴³ As a result, R_{O-H} was slightly elongated to 1.018 Å and R_{O-N} slightly reduced to 2.641 Å. The λ_{abs} of the $\pi\pi^*$ and $\pi\sigma^*$ transitions are 245 nm and 213 nm, which are almost consistent with those by PCM model. Based on the optimized structure, the PESs of S_0 and S_1 were obtained by gradually increasing R_{O-H} with freezing other coordinates since ESPT process is too fast to adjust structural relaxation. As shown in Fig 2 (c), the PESs obtained by explicitly treating water molecules in the first hydration shell resembled those obtained by PCM model. GSPT cannot take place due to the single well potential with PH-IM as most stable conformer, while ESPT can occur because P-HIM* is more stable than PH-IM* by ~ 1 kcal/mol and the energy barrier is about 3 kcal/mol. That is, solvent effect by PCM model was same as the result by explicit treatment of water. Hence, the followings were based on the results by PCM model to save computational cost. Due to the small barrier and relative stability, this ESPT reaction in solvent should be strongly influenced by the environment conditions, such as temperature, external electric field and so on.

Subsequently, the dipole moment of S_0 and S_1 both in vacuum and water was calculated along the phenolic proton transfer coordinate (in Fig 3). In both vacuum and water, the dipole moment of the ground state increased as the proton transfers. For S_1 in vacuum, the dipole moment increased from

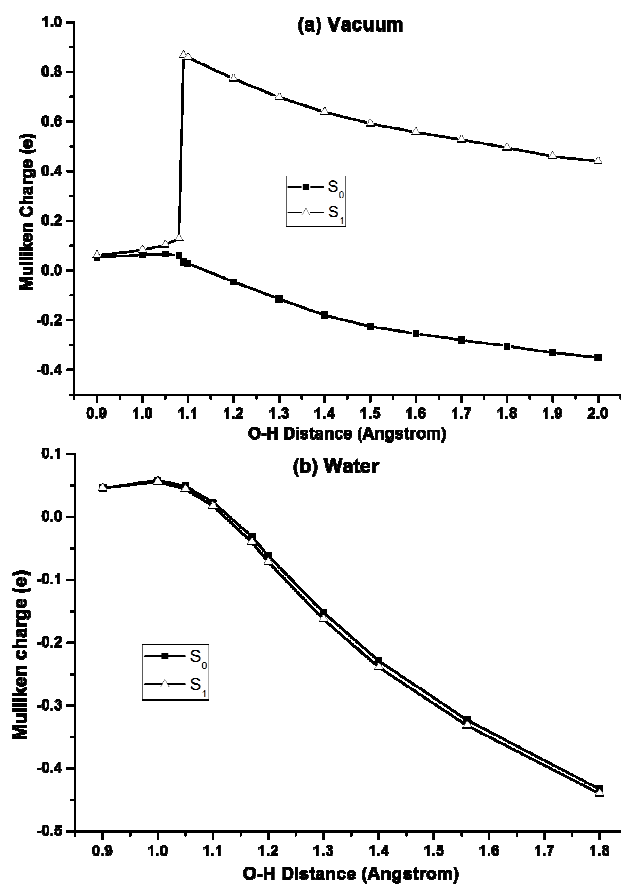


Fig 4. Group charge change of phenol along the O-H coordinate in (a) vacuum and (b) water.

7.0 D of PH-IM* to 8.4 D of TS*, then decreased to 4.4 D as the proton transfers to P-HIM*. The phenomena are similar to that of the phenol complexed with water in gas phase.³⁸ In addition, the dipole moment difference between S_0 and S_1 was small before reach TS/TS* in vacuum. After passing the TS/TS*, the dipole moment difference became larger as the proton transfers as shown in Fig 3(a). However, in water, the dipole moment of S_1 has a similar trend with that of S_0 as the proton transfers. To further elucidate this issue, the charge distribution was analyzed with/without solvent effect. Here we set the phenolate and the phenolic proton as a group, and obtained the group charge by the sum of the atomic charges of the atoms belonging to the group (Fig 4). In vacuum, as seen clearly, photo-induced charge separation did not occur until TS/TS*. After passing TS/TS*, the group charge became to be positively charged (0.8 e) in the excited state, which indicates an intermolecular electron transfer from the phenol to the imidazole moiety. Then it gradually decreased to ~ 0.5 e upon proton transfer. Thus, the reaction in vacuum is a proton coupled electron transfer (PCET) process. Moreover, the much smaller dipole moment of the P-HIM* in vacuum also originates from the charge separation during the proton transfer. However, no obvious charge separation upon excitation was observed in water. For the PH-IM/PH-IM*, the phenol was slightly positively charged (0.04 e). At the TS/TS*, it turned to be slightly negatively charged (-0.04 e). The behavior of the group charge of S_1 along the proton transfer process is almost equivalent to that of S_0 . After passing TS/TS*, the phenol moiety became to be negatively charged up to -0.3 e in P-

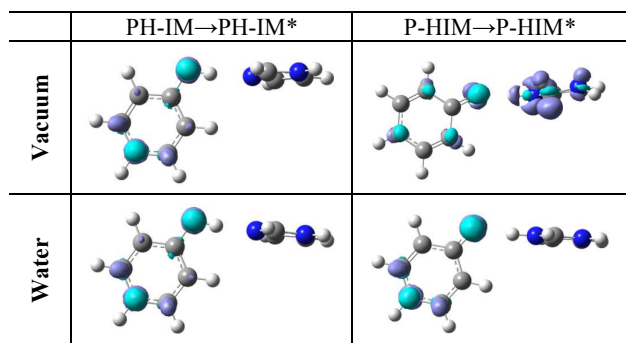


Fig 5. The electron density changes upon the first excitation for PH-IM and P-HIM both in vacuum and water (pale blue: electron density decrease, violet: electron density increase)

HIM/P-HIM*. Thus it turns out to be only a proton transfer reaction.

The difference in the behavior of charge distribution in vacuum and in water should originate from the MO reordering as solvent being applied. As confirmed by the MOs in vacuum, the first excitation corresponded to $\pi\pi^*$ transition before TS/TS*, and it turns to be $\pi\sigma^*$ transition after crossing TS (TS*). Differently from the case in vacuum, the first excitation in water corresponded to $\pi\pi^*$ transition. This phenomenon was previously observed in phenol-amine system.⁴⁴ There, the energy profile of the π^* state monotonously increases upon proton transfer in gas phase. When the solvent effect was taken into account, the PES of the π^* state changes from a single-well to a double-well curve with a small barrier (0.4~1.3 kcal/mol). Such change could be ascribed to the larger dipole moment of $\pi\pi^*$ state as reflected from Fig 3, which can be much stabilized to be the first excited state.

The electron density changes upon excitation obtained by Multiwfn program⁴⁵ were shown in Fig. 5. For PH-IM in vacuum and in water, the p electrons of O atom and C atom in para-position move to the C atoms in ortho- and meta-position upon excitation. Hence, the electron density of the oxygen decreases, meanwhile that of the benzene ring increases leading to an intramolecular CT process. This intramolecular charge transfer process destabilizes the hydroxyl group and makes it easier to detach the proton from phenol. It is noticeable that the electron density changes of P-HIM in vacuum and water are different. In vacuum, upon excitation the electron in phenol moiety moves to the imidazole ring inducing an intermolecular CT process. When solvent effect was applied, it turns to be an intramolecular CT process which is similar to PH-IM. In vacuum the transferred electron mostly localizes at the N atom H-bonded to phenol, which can further drive proton transfer. At the same time, it also induces the different structures of P-HIM* in vacuum and water.

Conclusions

A theoretical investigation of the hydrogen bonded phenol-imidazole complex in the ground state and the first singlet excited state was carried out. It was found that proton transfer does not take place in the ground state due to the single-well PES both in vacuum and in water. Under the excitation, the proton transfer can take place both in vacuum and in water, as determined by the energy barrier and the relative stability. Upon excitation both in vacuum and water, an intramolecular charge transfer in PH-IM from oxygen to the benzene ring happens, which would destabilize the hydroxyl group and make it easier to detach the proton of phenol. Under the attractive

force (characterized by the PA energy) of imidazole, proton transfer can take place. The energy barrier was calculated to be 1.09 kcal/mol in vacuum and 0.4 kcal/mol in water for the forward ESPT. For the reverse ESPT reaction, it cannot take place in vacuum because of the massive barrier, while it should be possible to happen due to the small energy barrier of 2.2kcal/mol. However, the reaction mechanisms in vacuum and in water are different. In vacuum, the first excitation changes from $\pi\pi^*$ to $\pi\sigma^*$ transition when crossing TS*, leading to an intermolecular charge transfer from phenol to imidazole to promote proton transfer. When the solvent effect considered, no such transition was observed and the first excited state always corresponds to the $\pi\pi^*$ transition. Such difference comes from the significant solvent effect on the π^* state which has large dipole. Due to the lack of intermolecular CT state, the geometry of P-HIM* in water differs from that in vacuum. In other words, it is an excited state proton coupled electron transfer (ESPCET) process in vacuum, while only PT reaction in water. As this is the first report on the excited state hydrogen transfer process of H-bonded phenol-imidazole complex, further experimental efforts are necessary to confirm these results. Even though this is a theoretical investigation, it should provide useful information in the study of photosystems.

Acknowledgements

This work was supported by the National Research Foundation of Korea (NRF) Grant (NRF-2012K1A2B1A03000362). This work was also supported by the Postdoctoral Research Program of Sungkyunkwan University (2014). S. Yan was supported by National Nature Science Foundation of China (Grant No.21203227), the Foundation for Outstanding Young Scientist in Shandong Province (No. BS2010NJ020), the Scientific Research Foundation for the Returned Overseas Chinese Scholars, State Education Ministry, and the Research Foundation for Talented Scholars of the Qingdao Agricultural University (No. 631335).

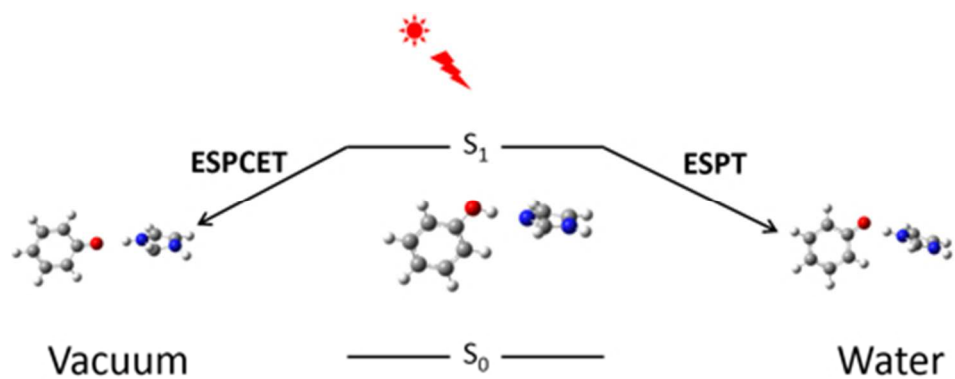
Notes and references

- ^a Department of Chemistry, Sungkyunkwan University, Suwon, 440746, Korea, *E-mail: jinylee@skku.edu
^b College Of Chemistry and Pharmaceutical Sciences, Qingdao Agricultural University, Qingdao, 266109, P. R. China, *E-mail: shyan@qau.edu.cn
[†] These authors equally contributed to this work.

Electronic Supplementary Information (ESI) available: Figures of initial structure of PH-IM in water box with cubic length of 22 Å for QM/MM calculation and behaviors of R_{O-N} and \angle_{COH} both in vacuum and water.. See DOI: 10.1039/b000000x/

- C. J. Chang, M. C. Y. Chang, N. H. Damrauer and D. G. Nocera, *Bba-Bioenergetics*, 2004, **1655**, 13-28.
- C. Costentin, M. Robert and J. M. Saveant, *J. Am. Chem. Soc.*, 2007, **129**, 5870-5879.
- R. I. Cukier and D. G. Nocera, *Annu. Rev. Phys. Chem.*, 1998, **49**, 337-369.
- S. Hammes-Schiffer, *Chemphyschem*, 2002, **3**, 33-42.
- J. Stubbe, D. G. Nocera, C. S. Yee and M. C. Y. Chang, *Chem. Rev.*, 2003, **103**, 2167-2201.
- P. E. M. Siegbahn and M. R. A. Blomberg, *Bba-Bioenergetics*, 2004, **1655**, 45-50.
- S. Y. Reece, J. M. Hodgkiss, J. Stubbe and D. G. Nocera, *Philos. T. R. Soc. B*, 2006, **361**, 1351-1364.

8. K. S. Kim, K. S. Oh and J. Y. Lee, *P. Natl. Acad. Sci. USA*, 2000, **97**, 6373-6378.
9. C. Tommos and G. T. Babcock, *Accounts. Chem. Res.*, 1998, **31**, 18-25.
10. S. FergusonMiller and G. T. Babcock, *Chem. Rev.*, 1996, **96**, 2889-2907.
11. S. Hammes-Schiffer, *Abstr. Pap. Am. Chem. S.*, 1998, **216**, U96-U96.
12. P. Faller, C. Goussias, A. W. Rutherford and S. Un, *P. Natl. Acad. Sci. USA*, 2003, **100**, 8732-8735.
13. J. P. McEvoy and G. W. Brudvig, *Chem. Rev.*, 2006, **106**, 4455-4483.
14. T. J. Meyer, M. H. V. Huynh and H. H. Thorp, *Angew. Chem. Int. Edit.*, 2007, **46**, 5284-5304.
15. B. A. Diner, *Bba-Bioenergetics*, 2001, **1503**, 147-163.
16. P. Faller, R. J. Debus, K. Brettel, M. Sugiura, A. W. Rutherford and A. Boussac, *P. Natl. Acad. Sci. USA*, 2001, **98**, 14368-14373.
17. G. Granucci, J. T. Hynes, P. Millie and T. H. Tran-Thi, *J. Am. Chem. Soc.*, 2000, **122**, 12243-12253.
18. J. Lorentzon, P. A. Malmqvist, M. Fulscher and B. O. Roos, *Theor Chim Acta*, 1995, **91**, 91-108.
19. S. S. Kim, M. Kim and H. Kang, *B. Korean Chem. Soc.*, 2009, **30**, 1481-1484.
20. Y. Qin and R. A. Wheeler, *J. Am. Chem. Soc.*, 1995, **117**, 6083-6092.
21. Y. Qin and R. A. Wheeler, *J. Phys. Chem. USA*, 1996, **100**, 10554-10563.
22. W. Siebrand and M. Z. Zgierski, *Chem Phys Lett*, 2001, **334**, 127-135.
23. W. Siebrand and M. Z. Zgierski, *Chem Phys Lett*, 2000, **320**, 153-160.
24. S. Yan, S. Kang, T. Hayashi, S. Mukamel and J. Y. Lee, *J. Comput. Chem.*, 2010, **31**, 393-402.
25. M. Sodupe, A. Oliva and J. Bertran, *J. Phys. Chem. A*, 1997, **101**, 9142-9151.
26. H. T. Kim, R. J. Green, J. Qian and S. L. Anderson, *J. Chem. Phys.*, 2000, **112**, 5717-5721.
27. M. Schmitt, C. Ratzler and W. L. Meerts, *J. Chem. Phys.*, 2004, **120**, 2752-2758.
28. P. J. O'Malley, *J. Am. Chem. Soc.*, 1998, **120**, 11732-11737.
29. P. J. O'Malley, *Bba-Bioenergetics*, 2002, **1553**, 212-217.
30. R. Kobayashi and R. D. Amos, *Chem Phys Lett*, 2006, **420**, 106-109.
31. T. Yanai, D. P. Tew and N. C. Handy, *Chem Phys Lett*, 2004, **393**, 51-57.
32. R. F. Li, J. J. Zheng and D. G. Truhlar, *Phys. Chem. Chem. Phys.*, 2010, **12**, 12697-12701.
33. D. A. Case, T. A. Darden, T. E. I. Cheatham, C. L. Simmerling, J. Wang, R. E. Duke, R. Luo, R. C. Walker, W. Zhang, K. M. Merz and e. al., AMBER12 2012, University of California, San Francisco
34. R. Salomon-Ferrer, A. W. Götz, D. Poole, S. Le Grand and R. C. Walker, *J Chem Theory Comput*, 2013, **9**, 3878-3888.
35. M. J. Frisch, G. W. Trucks, H. B. Schlegel, G. E. Scuseria, M. A. Robb, J. R. Cheeseman, G. Scalmani, V. Barone, B. Mennucci, G. A. Petersson, H. Nakatsuji, M. Caricato, X. Li, H. P. Hratchian, A. F. Izmaylov, J. Bloino, G. Zheng, J. L. Sonnenberg, M. Hada, M. Ehara, K. Toyota, R. Fukuda, J. Hasegawa, M. Ishida, T. Nakajima, Y. Honda, O. Kitao, H. Nakai, T. Vreven, J. A. Montgomery, Jr., J. E. Peralta, F. Ogliaro, M. Bearpark, J. J. Heyd, E. Brothers, K. N. Kudin, V. N. Staroverov, T. Keith, R. Kobayashi, J. Normand, K. Raghavachari, A. Rendell, J. C. Burant, S. S. Iyengar, J. Tomasi, M. Cossi, N. Rega, J. M. Millam, M. Klene, J. E. Knox, J. B. Cross, V. Bakken, C. Adamo, J. Jaramillo, R. Gomperts, R. E. Stratmann, O. Yazyev, A. J. Austin, R. Cammi, C. Pomelli, J. W. Ochterski, R. L. Martin, K. Morokuma, V. G. Zakrzewski, G. A. Voth, P. Salvador, J. J. Dannenberg, S. Dapprich, A. D. Daniels, O. Farkas, J. B. Foresman, J. V. Ortiz and a. D. J. F. J. Cioslowski, Gaussian 09, Revision B.01, Gaussian, Inc., Wallingford CT, 2010
36. L. Zhang, G. H. Peslherbe and H. M. Muchall, *Photochem Photobiol*, 2006, **82**, 324-331.
37. C. P. Schick and P. M. Weber, *J. Phys. Chem. A*, 2001, **105**, 3735-3740.
38. A. L. Sobolewski and W. Domcke, *J. Phys. Chem. A*, 2001, **105**, 9275-9283.
39. L. SerranoAndres, M. P. Fulscher, B. O. Roos and M. Merchan, *J. Phys. Chem. USA*, 1996, **100**, 6484-6491.
40. S. Chong, R. A. Myers and J. L. Franklin, *J. Chem. Phys.*, 1972, **56**, 2427-2430.
41. J. M. L. Martin and T. J. Lee, *Chem Phys Lett*, 1996, **258**, 136-143.
42. J. S. Rao and G. N. Sastry, *Int. J. Quantum. Chem.*, 2006, **106**, 1217-1224.
43. M. Shoji, H. Isobe, S. Yamanaka, Y. Umena, K. Kawakami, N. Kamiya, J. R. Shen and K. Yamaguchi, *Catal Sci Technol*, 2013, **3**, 1831-1848.
44. S. Aono and S. Kato, *J. Comput. Chem.*, 2010, **31**, 2924-2931.
45. T. Lu and F. Chen, *J. Comput. Chem.*, 2012, **33**, 580-592.



80x31mm (150 x 150 DPI)